ELSEVIER

Catalysis Today 72 (2002) 197–203

CATALYSIS TODAY

www.elsevier.com/locate/cattod

On the plasma-chemical synthesis and/or regeneration of ultradispersed catalysts for ammonia production

Gheorghi P. Vissokov*

Institute of Electronics, Bulgarian Academy of Sciences, 72 Tzarigradsko Chaussee Blvd, 1784 Sofia, Bulgaria

Abstract

The equilibrium compositions of multi-component heterogeneouse systems N–Al–O–Ca–Mg, Cu–Zn–Al–O and Fe–Al–K–Ca–Si–O in gaseous and condensed state are established. Further, we have developed a three-dimentional model dealing with the motion, heating, melting and evaporation (thermal destruction) of micron-size particles—(5–60 μm—Fe, Fe_2O_3, Fe_3O_4, FeO, Ni, NiO, Cu, Al, Al_2O_3, CaO, Mg, MgO) in an axial-symmetric plasma-chemical reactor (PCR). Based on the model calculations, we have designed and build plasma-chemical installations and used them to study the mechanisms of preparation of catalysts (and regeneration of spents of deactivated catalysts) for reforming of natural gas (steam conversion of CH_4), for low-temperature steam conversion of CO and for synthesis of NH_3.

A physical-chemical analysis of plasma-chemically synthesised (PCS) and/or regenerated ultra-dispersed catalysts in electric-arc low-temperature plasma conditions has been performed by X-ray structural and phase analysis, electron microscopy, Mössbauer spectroscopy, derivatographic, thermal-magnetic, chemical and analytical methods, by studing the dynamics and kinetics of formation of the active surface due to the reduction (the "plasma" catalysts undergo reduction 2–5 times faster than their respective commercial analoges and show activity by 15–20% higher than that of the conventional catalysts).

Keywords: Ultra-dispersed catalysts; Plasma-chemical synthesis; Regeneration; Properties; Reduction; Activity

1. Introduction

The two main trends in the plasma-chemical synthesis (PCS) of catalysts are: (1) plasma-chemical preparation and activation of catalysts in the condensed phase, and (2) plasma-assisted deposition of catalytically-active compounds and composites on various carriers [1]. The condensed-phase catalysts preparation can be carried out in both equilibrium (quasi-equilibrium) and non-equilibrium plasma conditions. The raw materials used can be either the compounds that make up the catalyst itself, (i.e. the plasma is only employed to disperse and activate the catalytic substances), or the catalysts can be synthesised during the plasma-chemical process (PCP). Furthermore, the ingredients are introduced in jet plasma-chemical reactors (PCR) as either a well-homogenised mechanical mixture of micron-size particles [1–5], or in the form of concentrated solutions and suspensions [6,7]. The plasma-chemical technique is also used for activation of spent deactivated catalysts [1–5,8]. Our pioneer works using the plasma-chemical approach and some fundamental results on PCS and/or regeneration of spent catalysts for ammonia synthesis [9–12] were commented on in Kizling and Jaras's review [8].

The patent, periodic and monographic literature available to us lacks data on the regeneration of exhausted, deactivated catalysts (and on the their synthesis,

* Fax: +359-2-9753201.
E-mail address: tfp@adm1.uctm.edu (G.P. Vissokov).

0920-5861/02/$ – see front matter
PII: S0920-5861(01)00493-X

in some case) for ammonia production processes: natural gas reforming (steam conversion of methane, SCM), low-temperature steam conversion of CO (LTSCCO) and NH_3 synthesis (AS).

The review of the specialised reference literature revealed also the absence of data on the values of the equilibrium parameters of the multi-component heterogeneous system Ni–Al–O–Ca–Mg, Cu–Zn–Al–O and Fe–Al–K–Ca–Si–O in the 1000–3700 K temperature range. These are the systems used to built the conventional catalyst for SCM, LTSCCO and for AS. Bearing in mind that modelling the physical and, possibly, the chemical processes taking place in PCR's is an important prerequisite for the design and development of highly-efficient plasma-chemical installations [13,14], we set out to develop a three-dimensional model for the motion and evaporation of micron-size particles in an axial-symmetric PCR, to determine the equilibrium parameters of the multi-component heterogeneous Ni–Al–O–Ca–Mg, Cu–Zn–Al–O and Fe–Al–K–Ca–Si–O systems for the plasma-temperature range, and to carry out experimental studies concerning the PCS of these catalysts.

The aim of this paper is to present our considerations and investigations about: the thermodynamic and kinetic peculiarities of PCP's for the preparation of ultradispersed catalysts (UDC) for ammonia production (for reforming of natural gas–steam conversion of CH_4, for low-temperature steam conversion of CO and for synthesis of NH_3); the three-dimentional models that describe the motion, heating, melting and evaporation (thermal destruction) of micron-size particles; the mechanism of evaporation of micron-size particles under the conditions of powder-carrier high-enthalpy chemically reactive plasma jets and the mechanism of condensation of UDC phases upon quenching; the correlation between the parameters of PCP occurring in powder carrier chemically-reactive high-enthalpy flows and the dispersity of the desired condensed UDC; the optimal PCP parameters (average mass temperature, type and geometry of plasma-chemical mixing chambers and reactors, quenching, trapping of condensed phases, etc.) in neutral, reducing, oxidising and redox media, leading to the obtaining of the desired condensed catalysts with controlled dispersity, chemical activity, phase composition, crystal lattice defects, etc.; the characterisation of some properties of PCS UDC (chemical, physicochemical, physical, catalytic, etc.).

2. Methods

2.1. High-temperature thermodynamics of the Ni–Al–O–Ca–Mg, Cu–Zn–Al–O and Fe–Al–K–Ca–Si–O systems

When calculating the variation of the free enthalpy of multi-component systems, we employed a technique that makes it possible to consider gaseous and condensed-phase compounds and solid solutions while allowing one to take into account the potential of electrostatic ionic interaction. We could, thus, follow in a large temperature interval (300–6000 K) a wide range of equilibria of the multi-component systems studied (Ni–Al–O–Ca–Mg, Cu–Zn–Al–O and Fe–Al–K–Ca–Si–O), beginning with the condensed state up to the plasma state. This technique also enabled us to use components at very low concentrations—down to 10^{-20} mol kg^{-1} [15].

2.2. Motion and evaporation of micron-size particles in an axial-symmetric cylindrical PCR

Devising three-dimensional models that describe the motion, heating, melting and evaporation (thermal destruction) of micron-size particles (5–60 μm—Fe, Fe_2O_3, Fe_3O_4, FeO, Ni, NiO, Cu, CuO, Al, Al_2O_3, CaO, Mg, MgO, Si, SiO_2) in an axial-symmetric cylindrical PCR is invaluable in obtaining sufficiently accurate data enabling one to determine the optimal PCP parameters: PCR size, time of residence of the particles in it, temperature and velocity profiles in a PCR with "cold" ($T_W = 500$ K) (CW) or "warm" ($T_W = 1500$ K) (WW) walls, the variation of the particles diameter and temperature along the PCR axis, etc. The theoretical and experimental studies of the processes mentioned are hampered by the short duration and the non-steady state and spatially non-uniform character of the accompanying phenomena, as well as by the multiple determining factors and their complex interdependence.

The equations we used to model the hydrodynamic and heat exchange-processes in a cylindrical axial-symmetric PCR were as follows:

2.2.1. A set of equations describing the gas motion (in cylindrical co-ordinates):

$$\frac{\partial \rho}{\partial t} + \frac{1}{r}\frac{\partial r(\rho v_r)}{\partial r} + \frac{\partial(\rho v_z)}{\partial z} = 0, \tag{1}$$

$$\frac{\partial(\rho v_r)}{\partial t} + \frac{1}{r}\frac{\partial r(\rho v_r v_r)}{\partial r} + \frac{\partial(\rho v_r v_z)}{\partial z} + \frac{\partial p}{\partial r} - \frac{1}{r}\frac{\partial(r t_{r,r})}{\partial r} - \frac{\partial(t_{r,z})}{\partial z} = 0 \tag{2}$$

$$\frac{\partial(\rho v_z)}{\partial t} + \frac{1}{r}\frac{\partial r(\rho v_z v_r)}{\partial r} + \frac{\partial(\rho v_z v_z)}{\partial z} + \frac{\partial p}{\partial z} - \frac{1}{r}\frac{\partial r(t_{z,r})}{\partial r} - \frac{\partial(t_{z,z})}{\partial z} = 0 \tag{3}$$

$$\frac{\partial \rho E}{\partial t} + \frac{1}{r}\frac{\partial r(\rho E w_r)}{\partial r} + \frac{\partial(\rho E w_z)}{\partial z} - \frac{1}{r}\frac{\partial r[(v_r t_{r,r}) + (v_z t_{z,r})]}{\partial r} - \frac{\partial[(v_r t_{r,z}) - (v_z t_{z,z})]}{\partial z} - \frac{1}{r}\frac{\partial}{\partial r}\left(rk\frac{\partial T}{\partial r}\right) - \frac{\partial}{\partial z}\left(k\frac{\partial T}{\partial z}\right) = \sigma b T^4, \tag{4}$$

where the relation between the energy (E), pressure (p), velocity (v_z, axial and v_r, radial) and density (ρ) is given by $E = p/\rho(\gamma - 1) + \frac{1}{2}|\vec{v}|^2$; also, $w_{x\,\mathrm{or}\,z} = v_{x\,\mathrm{or}\,z}(1 + p/\rho E)$; k is the heat-conduction coefficient; γ the adiabatic index; σ the Stefan–Boltzmann constant of black-body radiation; b the blackness coefficient; and Newton's viscosity tensor has the form:

$$t_{r,r} = 2\mu\frac{1}{r}\frac{\partial r v_r}{\partial r} - \frac{2}{3}\mu\left(\frac{1}{r}\frac{\partial r v_r}{\partial r} + \frac{\partial v_z}{\partial z}\right),$$

$$t_{r,z} = t_{z,r} = \frac{2}{3}\mu\left(\frac{1}{r}\frac{\partial r v_z}{\partial r} + \frac{\partial v_r}{\partial z}\right),$$

$$t_{z,z} = 2\mu\frac{\partial v_z}{\partial z} - \frac{2}{3}\mu\left(\frac{1}{r}\frac{\partial r v_r}{\partial r} + \frac{\partial v_z}{\partial z}\right), \tag{5}$$

where μ is the dynamic viscosity. Equations for the particle temperature T_p as a function of the gas temperature T_g:

$$m_\mathrm{p} C_p \frac{\mathrm{d}T_\mathrm{p}}{\mathrm{d}t} = \alpha_\mathrm{T} S_\mathrm{p}(T_\mathrm{g} - T_\mathrm{p}), \quad \text{for } T_\mathrm{p} < T_\mathrm{m} \tag{6}$$

$$m_\mathrm{p} L_\mathrm{m} = \int_{\Delta t} \alpha_\mathrm{T} S_\mathrm{p}(T_\mathrm{g} - T_\mathrm{p})\,\mathrm{d}t, \quad \text{for } T_\mathrm{p} = T_\mathrm{m} \tag{7}$$

$$m_\mathrm{p} C_p \frac{\mathrm{d}T_\mathrm{p}}{\mathrm{d}t} - L_\mathrm{v}\frac{\mathrm{d}m_\mathrm{p}}{\mathrm{d}t} = \alpha_\mathrm{T} S_\mathrm{p}(T_\mathrm{g} - T_\mathrm{p}), \quad \text{for } T_\mathrm{p} < T_\mathrm{v} \tag{8}$$

$$-L_v\frac{\mathrm{d}m_\mathrm{p}}{\mathrm{d}t} = \alpha_\mathrm{T} S_\mathrm{p}(T_\mathrm{g} - T_\mathrm{p}), \quad \text{for } T_\mathrm{p} = T_\mathrm{v} \tag{9}$$

where T_m, T_v, L_m and L_v are the temperatures and heats of melting and evaporation, respectively; C_p the specific heat of the particle; m_p, S_p the mass and surface of the particle; and α_T the heat-transfer coefficient ($\alpha_\mathrm{T} = \lambda_\mathrm{g}/r_\mathrm{p} Nu/2$, r_p being the radius of the particle and λ_g, the heat conductivity of the gas).

Equation for the motion of the particle

$$m_\mathrm{p}\frac{\mathrm{d}\vec{V}_\mathrm{p}}{\mathrm{d}t} = \frac{1}{2}C_\mathrm{D} S_\mathrm{p}\rho_\mathrm{g}|V_\mathrm{g} - V_\mathrm{p}| \cdot (\vec{V}_\mathrm{g} - \vec{V}_\mathrm{p}), \tag{10}$$

where ρ_g is the plasma (gas) density; C_D the dra coefficient; and V_g and V_p the velocities of the gas and the particle, respectively.

3. Experimental

Based on the model calculations, we have designed and build plasma-chemical installations and used them to study the processes of preparation of catalysts and regeneration of spent of deactivated catalysts for SCM, LTSCCO and for AS. One of them is shown schematically in Fig. 1.

The consumption of the powder ingredients was 2–3 g min^{-1} depending on the amount of the powder-carrying gas and on the piston revolution rate of the vibration powder-feeding device. The equipment's output was within the 100–150 g h^{-1} range. Ar was used as a plasma-forming gas, while O_2 and H_2 were both—a powder-carrying gases and an oxidative (O_2), or reducing (H_2) agents. Temperature in the PCR was determined by calorimetry.

The samples of catalysts were characterised by their specific surface area measured using the BET technique, bulk mass and chemical content; spectral emission, derivatographic, X-ray structural and phase analysis, Mössbauer spectroscopy, electron microscope, etc. analyses were performed for this purpose. The dynamics and kinetic of reduction and the catalytic activity were followed using the flow technique.

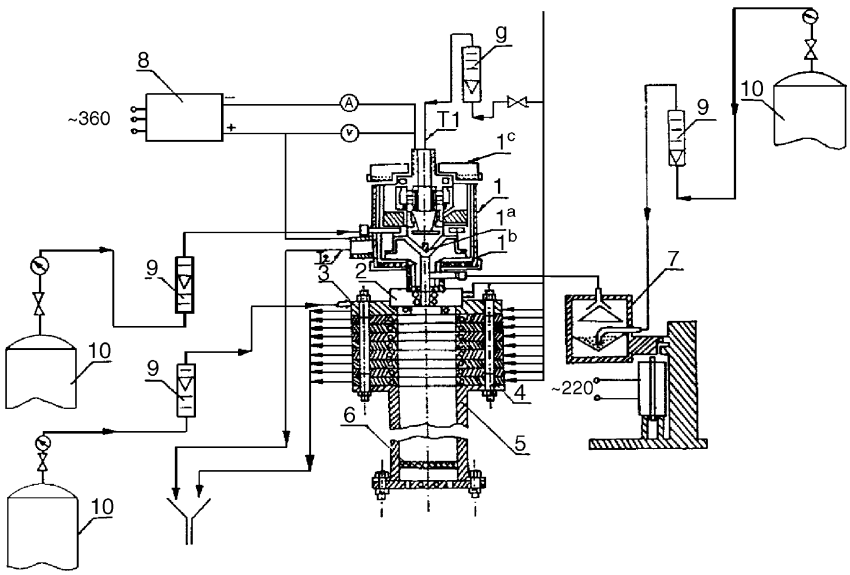

Fig. 1. Schematic diagram of plasma-chemical installation for synthesis and/or regeneration of UDC for ammonia production: (1) electric-arc dc plasmatron; (1a) thoriated tungsten cathode; (1b) copper water-cooled anode; (1c) plastic adjusting ring; (2) CW PCR; (3) quenching device; (4) copper water-cooled sections of the quenching device; (5) powder-trapping chamber; (6) filter; (7) vibration powder-feeding device (if necessary, a piston type vibration powder-feeding device can also be used); (8) current rectifier; (9) flow-rate meters; (10) bottles with plasma-forming, powder-carrying and quenching gases. T_1: temperature of inlet water, T_2: temperature of outlet water.

4. Results and discussion

Tables 1 and 2 summarises some technological parameters (optimal temperature range) and properties (specific surface) of plasma-chemical treatment of the Ni–Al–O–Ca–Mg, Cu–Zn–Al–O and Fe–Al–K–Ca–Si–O systems in oxidative medium (Table 1) and in reducing-oxidative medium (Table 2).

4.1. PCS and/or regeneration of catalysts for SCM

PCS and/or regenerated samples have homogenous chemical composition similar to that of Girdller (USA) conventional industrial catalyst. It is empirically established that the optimal temperature range in PCR for synthesis of maximum dispersity samples is 2000–3000 K (Table 1).

Results from investigation on plasma-chemically synthesised and/or regenerated SCM catalysts dynamics and kinetics show that under low-temperature plasma (LTP) conditions premises for catalyst compositions formation are established. We found that the PCS samples were reduced 3–4 times as fast as the conventional G56A catalyst. The synthesised and regenerated SCM catalyst have a commensurable activity to that of G56A industrial sample (Table 3).

The high catalytic activity of the plasma-chemically synthesised SCM catalysts is a result of the high

Table 1
Plasma-chemical processes developed for UDC production in oxidising medium—synthesis or regeneration of catalysts

Basic reaction	UDP: specific surface area ($m^2\,g^{-1}$)	Temperature range (K)
(Ni, Al) + O_2 ⇒ NiO + Al_2O_3 + $NiAl_2O_4$	Catalysts for SCM; up to 110	2000–3000
(Cu, Zn, Al) + O_2 ⇒ CuO(Cu_2O) + ZnO + Al_2O_3	Catalysts for LTSCCO 45–51	Up to 5100
$3Fe + 2O_2 \Rightarrow Fe_3O_4$	Catalysts for AS up to 40	1100–3400
$4Fe + 3O_2 \Rightarrow Fe_2O_3$	Catalysts for AS up to 40	1100–3400
$2Fe + O_2 \Rightarrow 2FeO$	Catalysts for AS up to 40	1500–3500

Table 2
Plasma-chemical processes developed for UDC production in reducing–oxidizing medium

Basic reaction	UDC: specific surface area ($m^2\,g^{-1}$)	Temperature range (K)
$NiO + H_2 \Rightarrow Ni + H_2O$ (I)	Catalysts for SCM up to 40	$(1–4) \times 10^3$
$2Ni + O_2 \Rightarrow 2NiO$ (II)	Catalysts for SCM up to 40	$(4–1) \times 10^3$
$(CuO, ZnO, Al_2O_3) + H_2 \Rightarrow (Cu, Zn, Al) + H_2O$ (I)	Catalysts for LTSCCO; up to 50	$(1–4) \times 10^3$
$(Cu, Zn, Al) + O_2 \Rightarrow CuO(Cu_2O) + ZnO + Al_2O_3$ (II)	Catalysts for LTSCCO; up to 50	4×10^3 to 300
$Fe_3O_4 + 4H_2 \Rightarrow 3Fe + 4H_2O$ (I)	Catalysts for AS; 10–30	$(1–4) \times 10^3$
$3Fe + 2O_2 \Rightarrow Fe_3O_4$ (II)	Catalysts for AS; 10–30	4×10^3 to 30

Table 3
Catalyst activity in natural gas reforming process and some main process parameters

N	V (h^{-1})	Converted gas composition (vol.%)				CH_4 conversion rate, η (%)	Catalyst performance[a]	Catalyst efficiency (η_{ef})
		CO_2	CO	H_2	CH_4			
Conventional G56A catalyst ($T = 923$ K)								
1	2000	13.0	3.9	63.7	13.3	80.6	1352	99.5
2	5000	11.5	2.4	53.2	32.9	67.1	2780	82.8
3	7500	11.2	2.2	51.4	35.2	64.8	4020	80.0
4	10000	11.1	2.1	50.7	36.1	63.9	5280	78.9
PCS catalyst ($T = 923$ K)								
5	2000	13.0	3.7	63.1	20.2	79.8	1336	98.5
6	5000	11.9	2.9	56.3	28.9	71.1	2960	87.8
7	7500	11.4	2.5	54.3	31.8	69.2	4260	84.2
8	10000	11.3	2.3	52.7	33.7	66.3	5500	81.9
Conventional G56A catalyst ($T = 873$ K)								
9	2000	10.1	1.0	43.4	45.5	54.5	888	91.0
PC regenerated catalyst ($T = 873$ K)								
10	2000	10.2	1.0	43.8	40.0	59.0	896	98.6

[a] $G \times 10^3[m^3(CO + H_2)]m_{cat}^{-3}$.

sample specific surface (to $110\,m^2\,g^{-1}$) and of the high particles dispersity (10–40 nm), faulty structure and phase composition defined upon condensed phase forming after PCR at a quenching velocity of $dT/d\tau \cong 10^4$–$10^5\,K\,s^{-1}$; NiO homogenous distribution between structure-stabilising Al_2O_3 and activating CaO, and not in the last place their temperature-resistance is determined by the existence of $NiAl_2O_4$ in the fresh samples.

4.2. PCS and/or regeneration of catalysts for LTSCCO

The WW PCR synthesised LTSCCO catalyst samples show activity similar to their industrial analogues; and these synthesised in PCR with CW have a commensurable activity compared to those of the industrial catalysts used by the Bulgarian company CHIMCO-Vratza. The catalysts synthesised by us are more active than their analogues synthesised by some Russian scientists [1–6]; and there is no other literature data on that problem in the reference licensed and periodical literature on this stage.

The equilibrium parameters of the multi-component heterogeneous system Cu–Zn–Al–O in two variants of the initial ingredient composition at pressure of 0.1 MPa within the temperature range from 1000 to 3700 K are defined by use of a universal programme. Dependencies of the concentration of the corresponding compound in gas and condensed phase at an equilibrium composition of the system on the temperature are found [15].

The conditions and the process parameters of the PCS and/or regeneration of catalysts for low-temperature steam conversion of CO under the conditions of electric-arc LTP are investigated, as depending on the PCP parameters and the PCR type (with CW or WW). Samples that have the following properties are obtained: specific surface area, up to $56\,m^2\,g^{-1}$; particle sizes, 10–60 nm, in some cases up to 200 nm; faulty crystal lattice structure; phases of ZnO, CuO, Cu_2O and $CuAl_2O_4$.

This is the first time worldwide, when an attempt to regenerate already processed, deactivated catalysts for low-temperature steam conversion of CO is made. The conditions for plasma-chemical regeneration of already processed catalyst of *Loyna-1961* (GDR) type stayed for 2–3 years in the open air are investigated. The regenerated samples display a low specific surface area ($10–12\,m^2\,g^{-1}$) and a catalytic activity that is owing to: the caking and the agglomeration of the ultra-dispersed particles; the presence of an unreacted coarse-dispersed elemental Cu; the availability of a hardly reactable spinel ($CuAl_2O_4$); the unstable, in some cases, operating conditions of the electric-arc plasmotron.

It is experimentally proved that the optimal temperature range in the PCR for synthesis of samples with maximum dispersity and catalytic activity is from 2000 to 3800 K.

A complex physicochemical analysis of the plasma-chemically synthesised and/or regenerated samples by the following methods is performed: X-ray diffraction patterns, electron-microscope, chemical and other analyses. Samples activities are defined by using a model gas, simulating the industrial one, for temperatures and volume rate of the steam–gas mixture similar to those used in the low-temperature steam conversion of CO industrial process.

The WW PCR synthesised catalyst samples have activity similar to their industrial analogues and these synthesised in PCR with CW have a commensurable activity compared to those of the industrial catalysts used by the Bulgarian company CHIMCO-Vratza.

The enhanced catalytic activity of the plasma-chemically synthesised samples is owing to: the faulty crystal lattice structure of the catalytically active phases; the ultra-dispersed sample composition (the crystal sizes of the catalytically active phases range from 10 to 40 nm); the presence of Cu_2O in the fresh samples, apart from the presence of CuO; the content of cuprous oxides, 30–38 mass%; the even distribution of the ultra-dispersed components, the high porosity, specific surface area and dispersity of the phases (Tables 1 and 2).

Due to the bonding of a portion of the elemental Cu in the $CuAl_2O_4$ spinel crystal lattice, the plasma-chemically synthesised samples of LTC type have a high thermal resistance which exceeds that of their conventional industrial analogues.

The high specific surface area of the plasma-chemically synthesised samples for low-temperature steam conversion of CO; their homogenous chemical composition; high formation rate of their active surface by reduction; high activity and thermal resistance; all that represent a precondition to extend the investigation on developing a plasma-chemical technology for their industrial synthesis in the catalyst work-shops.

4.3. PCS and/or regeneration of catalysts for AS

AS catalysts with a specific surface area up to $40\,m^2\,g^{-1}$ (with a dominant fraction up to 100 nm; on regeneration 100–300 nm), (Tables 1 and 2) have been obtained, with main phases Fe_3O_4, Fe_2O_3, FeO, $FeO{\cdot}Al_2O_3$, α-Fe, γ-Fe. The above-mentioned composition and data is taken from the X-ray diffraction analysis of the samples and the Mössbauer spectra.

Active surface formation dynamics and kinetics have been studied by reduction on a line plant at pressure of 0.1 MPa; and the activity at 0.1 and 30 MPa at volume rate of stoichiometric nitrogen–hydrogen mixture. Test samples activity is by 15–20% higher than that of the conventional catalyst type CA-1 [14,15]. The relative rate of conversion, rate constants, activating energies on kinetic and diffusion control of the process, relative activities, the rate of conversion on deactivation and other parameters are determined. It is experimentally proved that the optimal temperature range in a PCR for synthesis of maximum activity and dispersity samples, is 1300–3000 K.

The mechanism of plasma-chemical regeneration of catalysts is as follows. In a PCR, a significant portion of the catalyst particles mass is in gas phase. The efficient quenching with a rate of $dT/d\tau \cong 10^5$–$10^6\,K\,s^{-1}$ brings the catalyst mass in condensed phase out of the system with a rate that does not allow a normal building of crystal lattices of its forming components. The

catalyst poisons (for instance oils) leave the system in the form of volatile gas products.

Deactivated already processed catalyst contains also elemental Fe (according to data taken from the Mössbauer spectra it is up to 90%), which is fixed in the unstable γ-modification the α-Fe by the thermal shock on quenching. A catalyst with almost the same Fe^{2+}:Fe^{3+} ratio, with a big specific surface area (10–30 $m^2\ g^{-1}$) and a lot of defects in the ferrous/ferric oxides crystal lattice on complete bounding of Al_2O_3 in the form of $FeO{\cdot}Al_2O_3$ (that determines the high thermal resistance of the regenerated samples) is formed.

It is reported a relative variation in *a*, the parameter of the ferrous/ferric oxides crystal lattice within the composition of UDP up to 0.9 rel.%, which is due to two oppositely acting factors. On one hand, the Laplas pressure (for UDP with sizes <30 nm) aims to reduce the interatomic distance within the crystal lattice. On the other hand, the impurity atoms on implantation lead to an increase of the interlayer distances. So, for instance, the Mössbauer spectra analysis of the sample promoted by K_2O and Al_2O_3, synthesised under the conditions of LTP, witnesses that Al_2O_3 is implanted into the Fe_3O_4 crystal lattice and increases the quantity of ferric ions in the tetrahedral coordination towards the stoichiometric quantity. That implantation impacts on the faultiness of the Fe crystal lattice after reduction. There are also found adequate compositions of the passivating gas mixtures for prevention of the samples pyrophority after reduction.

Within the framework of the complex physicochemical investigation on the samples, a thermomagnetic analysis by the compensation ballistic method is performed. For low values of the magnetising field, the Hoppckinson effect is observed. The Curie temperature of the reduction samples depends on the composition and their reduction degree, and that of the unreduced catalysts is determined by the formation of solid solutions with the ferrous/ferric oxides. The thermal magnetic hysteresis of the catalysts depends on the reduction degree, highest heating temperature of the samples, heating and cooling temperature, as the chemical interactions and the crystallographic conversion in the catalysts have a significant impact.

Using the method of Delmon [16] for layer gradual dissolution of the UDC surface, it is shown that the elemental impurities are distributed in conformity with the a priori concept of consecutive condensation of the components, depending on the respective values of the condensation (boiling) temperature. Higher-boiling impurities are situated in the bulk of UDC (e.g. W) while impurities condensing at lower temperature are found on the surface (e.g. K_2O in UDP of the catalyst for AS).

5. Conclusion

High specific surface area of the PCS catalysts, homogenous composition, high rate of active chemical surface forming by reduction, faulty crystal lattice of catalytically active phases and mostly high catalytic activity make them a potential competitor of their industrial analogues upon their probable production in catalyst shops.

References

[1] G.P. Vissokov, Commun. Dept. Chem. Bulg. Acad. Sci. 16 (1983) 114.
[2] G.P. Vissokov, Applied Plasmachemistry, Pt. 1, Low-temperature Plasma, Application in Inorganic Technologies, Sofia, Tekhnika, 1984, p. 295.
[3] G.P. Vissokov, Applied Plasmachemistry (Bulgaria), Pt. 2, Low-temperature Plasma, Application in Organic Technologies and Metallurgy, Sofia, Tekhnika, 1987, p. 325.
[4] G.P. Vissokov, Commun. Dept. Chem. Bulg. Acad. Sci. 16 (1983) 275.
[5] G.P. Vissokov, D.Sc. thesis, Institute of Electronics, Bulgarian Academy of Sciences, Sofia, 1994, p. 385.
[6] P. Tsibulev, D.Sc. thesis, Institute of Inorganic Chemistry, Ukrane Academy of Sciences, Kiev, 1996.
[7] P. Tsibulev, V. Parhomenko, Katalis and Katalizatory, Naukova Dumka, Kiev, 1989, p. 17.
[8] M. Kizling, S. Jaras, Appl. Catal. A Gen. 147 (1996) 1.
[9] T. Peev, G. Vissokov, I. Czako-Nagy, A. Vertes, Appl. Catal. 19 (1985) 301.
[10] G. Vissokov, T. Peev, I. Czako-Nagy, A. Vertes, Appl. Catal. 27 (1986) 257.
[11] G. Vissokov, Latvian J. Chem. 6 (1992) 662.
[12] G. Vissokov, Latvian J. Chem. 3 (1992) 334.
[13] P. Pirgov, G. Vissokov, Khimiya I Industriya Sofia 67 (1996) 54.
[14] G. Vissokov, P. Pirgov, in: A. Andreev, L. Petrov, Ch. Bonev, G. Kadinov, I. Mitov (Eds.), Proceedings of the 8th International Symposium on Heterogeneous Catalysis, Varna, 1996, Pt 2, Acad. Publ. House, Sofia, 1996, p. 763.
[15] G. Vissokov, P. Pirgov, Ultradispersed Powders, Plasmachemical Synthesis and Properties, Polyprint, Sofia, 1998, p. 396.
[16] B. Delmon, Kinetics of Heterogeneous Reactions (Russian), Mir, Moscow, 1972, p. 554.